

Available online at www.sciencedirect.com**ScienceDirect**

Energy Procedia 36 (2013) 574 – 590

Energy

Procedia

The effects of organoclay on the morphology and balance properties of an immiscible Polypropylene/Natural Rubber blend

C. Bendjaouahdou,^{a*} S. Bensaad^b^a *Department of chemical engineering, Med Khider -Biskra University, Algeria.*^b *Department of Chemistry, Mentouri-Constantine University, Algeria.*

Abstract

The objective of this work is to study the effects of organoclay on the morphology and balance properties between strength and toughness of a blend based on polypropylene (PP) and natural rubber (NR). This nanocomposite blend (nanoblend) was prepared by melt extrusion technique. The results obtained show that at 3 wt % organoclay concentration there is a slight balance between strength and toughness of the blend. On the other hand, the results obtained by XRD analysis show that, at 3 wt % of organoclay loading, there is a shift towards low angles of the (001) plane diffraction peak. This shift means an intercalation of the macromolecular polypropylene/natural rubber blend chains between the clay platelets. The SEM study reveals that at 3 wt % organoclay concentration there is a uniform distribution of the elastomeric dispersed domains. TGA analysis revealed an improvement of the thermal stability of the composite containing 3 wt % organoclay. DSC study shows that at 3 wt % organoclay concentration, there is a decrease of the melting temperatures of the blend; this decrease can be explained by the intercalation of NR chains between organoclay platelets. This intercalation can hinder or disturb the physical transition of the intercalated PP chains. The simultaneous intercalation of PP and NR chains into organoclay galleries can be explained by the localization of the organoclay platelets at the interface between PP and NR domains as assessed by SEM examinations

Keywords : nanocomposite; organoclay; polypropylene; natural rubber; XRD; SEM; DSC.

* Corresponding author : Tel.:+0-213-033 745 -174

E-mail : Chawk052000@yahoo.fr

© 2013 The Authors. Published by Elsevier Ltd. Open access under [CC BY-NC-ND license](http://creativecommons.org/licenses/by-nc-nd/4.0/).
Selection and/or peer-review under responsibility of the TerraGreen Academy

1. Introduction

Most of studies on polymer/clay nanocomposite preparations claim applicability of the invented method to a variety of polymers and their blends [1, 2]. Furthermore, some focus on the use of blends as a matrix for the modification of performance, e.g., improving stiffness, permeability control, or a good balance of performance [3]. For example, Chen and co-workers [4] have prepared a nanoblend with PU/PCL and ADA modified montmorillonite, they have found that tensile strength and modulus increased linearly with clay content. Other publications reported the compatibilizing effect of organoclay on immiscible polymer blends [5, 6]. Ray and co-worker [7] have studied the role of organoclay both as a compatibilizer and nanofiller in PS/PP and PS/PP-g-MA blends. They have found that when adding organoclay there is a reduction of the domain size of the dispersed phase and the mechanical properties were improved.

Thermoplastic elastomers (TPEs) are a new class of thermoplastic materials which are based on an elastomer and a plastomer and their properties can be more easily tailored by simply changing the ratio of the rubber to plastomer in the blend. They possess the elasticity of a rubber and the thermoplasticity of a plastic, yet retain unique features of its components such as better ultraviolet and ozone resistance, solvent resistance and high deformation temperature compared to some elastomers [8]. Furthermore, they can be processed by extrusion, injection moulding or blow moulding processes to provide commercially attractive products that show the softness, extensibility and resilience of thermoset rubbers. The most important feature of this class of material is that the scrap can be recycled up to several times without significant loss of properties. As a result, many commercial TPEs have been developed for various applications in the automotive, electrical and medical industries. Most polyolefin TPEs are based on synthetic rubbers such as ethylene-propylene-diene monomer (EPDM), styrene-ethylene-butylene-styrene (SEBS), ethylene propylene rubber (EPR) and butadiene acrylonitrile rubber (NBR) or a modification of them. Generally, it is easy to combine a rubber and a thermoplastic of similar polarities and solubility parameters to produce a useful thermoplastic elastomer, such as polypropylene (PP)/ ethylene-propylene-diene monomer (EPDM), Poly (vinyl chloride) (PVC)/butadiene acrylonitrile rubber (NBR) and nylon/NBR. Polypropylene (PP)/natural rubber (NR) blends have been studied due to the high melting temperature of PP meeting the dimensional stability at elevated temperatures of NR [9].

However it is difficult to produce a TPE using a plastic and an elastomer having different polarities and solubility parameters. This is due to the existence of a high interfacial tension between the two polymers. This problem can be overcome by the use of a compatibilizer to improve the interfacial adhesion between the two phases [8]. One way of improving the properties of a polymeric blend is to introduce filler into the system [10]. Addition of fillers is favoured because it is a cheap, effective and a fast method to modify the properties of the base material. The degree of improvement often depends on the type of the filler (synthetic or natural), particle size and shape, filler content and surface treatment which promotes interaction between the filler and the polymer matrix [11]. For industrial applications, the elastomeric components are added to the thermoplastic polymers in a proportion which varies generally from 5 to 15 % wt, and this, in order to improve the elasticity properties (ductility and impact resistance)[12].

The main objective to add organoclay to a thermoplastic elastomer blend is to improve the mechanical properties (stiffness and hardness) because the adding NR or other elastomeric component to a thermoplastic component (such as PP) increases the toughness (impact strength) but unfortunately decreases the stiffness (tensile modulus), strength and hardness of the resulting blend [13-15].

The addition of up 3 % wt of an organoclay to a 70/30 PA6/SEBSgMAH blend led to a thermoplastic elastomer combining the stiffness improvement due to the inclusion of organoclay and the toughening

effect of the rubber component [16]. The Interest to combine the natural rubber (NR) and a thermoplastic polymer has increased recently because of abundance of NR and its low cost.

To date no study related to the study the effects of organoclay in a thermoplastic elastomer blend containing isotactic polypropylene (iPP) and SMR- ω grade natural rubber (SMR- ω NR) was found in the literature. The aim of this work is to study the effects of organically modified montmorillonite (OMMT) both as compatibilizer (able to produce a uniform morphology and to improve the ductility or elongation at break) and a nanofiller (able to improve the strength and hardness) in a thermoplastic elastomer blend based on iPP and SMR- ω NR. The organoclay concentration was varied from 0 to 9 phr. The PP/NR weight ratio was set equal to 90/10 because it is a mean value used for industrial applications [12] and academic research [17].

2. Experimental

2.1. Materials

A commercially available isotactic polypropylene (trade marked as: ω 34-981903908, produced by APPRYL SNC France) with $M_w/M_n=4$, a melting temperature of 169 °C, a melt flow index (MFI) equal to 0.148 g/min (measured at 190°C under 2.16 Kg load), was used as the blend major component. The natural rubber used (SMR- ω grade) was purchased from Akrochem Corp, with a Mooney viscosity of ML (1+4) = 130, and it was not crosslinked.

The reinforcement used is BENTONE 38[®] (BENTONE SUD, France), it is an organically modified montmorillonite (OMMT) clay and it was used, as received, without washing (Cationic Exchange Capacity = 120 mEq/100g). As mentioned by the manufacturer, the quaternary ammonium salt used for the clay organic modification is: Di-Methyl Di-Hydrogenated Tallow salt: 2M2HT (HT = C₁₈H₃₇). The concentration of the quaternary ammonium salt ranged from 15 to 30 wt %. The organoclay was in powder form with a 20 μ m mean dry particle size.

2.2. Preparation of the samples

Before blending, clay and polypropylene were dried in oven at 80 °C during 24 hours. The components were melt blended, at 175 °C, in a two roll mill (BRABENDER POLYMIX 200P). The twin roll mill possesses a nip clearance of 0.5 mm and friction ratio equal to 1.3 (20/15 rpm) and the blending was carried out for 15 minutes. We began by mixing polypropylene (PP) and natural rubber (NR) on the two roll mill, for 10 minutes; afterwards, the clay was added for 5 minutes. Finally, the blend was extruded in a single screw extruder. The extruder used is SCHWABENTHAN PLE 330; it has a ratio length/diameter equal to 21, a diameter of 20 mm, a thread thickness of 5.4 mm and the step between two successive threads equal to 15 mm. The barrel temperatures (from feed zone to die) and screw speed were set, respectively, at 170-180-190 °C and 45 rpm. The screw used is conventional. Six formulations have been studied. In each formulation the weight ratio PP/NR was kept constant and equal to 90/10.

2.3. Characterizations

Tensile tests were done at ambient temperature ($25 \pm 2^\circ\text{C}$) according to ASTM D 417 with a ZWICK ROELL Z100 testing machine interfaced with a computer. The dumb-bell shaped specimens were extended at a cross head speed of 100 mm/min. The reported values of the tensile properties represent averages of the results from test runs on five specimens. The standard deviation was 3 % for Young's modulus, 2 % for the maximal tensile strength, and 5 % for the elongation at break.

The dumb-bell shaped specimens (gauge length 24 mm, width 5 mm, thickness 2 mm) were cut with a special cutting machine from sheets having 2 mm thickness. These sheets were obtained by compression moulding 35 g of each sample at 175 °C in a SCHWABENTHAN POLYSTAT 300S hydraulic press, according to the following program : preheating during 7 minutes; 50 Bars pressure applied for 2 minutes; 200 Bars applied for 3 minutes and finally, 350 Bars applied for 4 minutes.

Izod impact strength values of the composites were evaluated with a CEAST RESIL impact test instrument with a pendulum of 1 with a speed of 3.46 m/s J according to the ASTM D-256 test procedure at room temperature. Izod impact tests were performed for notch tip radius of 1 mm on notched rectangular strips of 12.5 x 3.2 x 62 mm³. At least five measurements were carried out and average values are reported for each blend. The standard deviation for the Izod impact strength was 8 %. All samples before to be tested, were conditioned for 24 hours, under relative humidity of $55 \pm 5 \%$ at $25 \pm 2 \text{ }^{\circ}\text{C}$ according to ISO 291 norm.

Shore A hardness tests were carried out by ZWICK ROELL HPE apparatus according to ISO 868 norm. It was done by six measurements on each side of a 3 mm thick plate obtained by compression moulding. These measurements were then averaged. The standard deviation for the Shore A hardness was 3 %.

X-ray diffraction measurements (WAXD) were conducted on Xpert Philips diffractometer, interfaced with computer, operating at 40 KV and 40 mA in a continuous mode. The incident ray has a wavelength equal to 1.54 Å, generated by CuK_α anode. The 2 θ range was 1.51 to 19.99 ° with a scanning rate of 0.02 °/min. The composite specimens analysed by X-ray diffraction were films, having 0.5 mm thick, obtained by compression moulding at 175°C.

The SEM study was done with a Hitachi S-3600N apparatus operating at an acceleration voltage of 15 KV on a BSE (Back Secondary Electron) and SE (Secondary Electron) mode. The cross sections of the samples fractured in the tensile tests were examined and the elastomeric phase was not extracted. For every samples, when taking micrographs a minimum of three frames at each magnification were taken to ensure confidence in the analysis.

The thermal stability of the PP/NR/clay composites and PP/NR were investigated by thermogravimetric analysis (TGA) performed with a TA SDT Q600 apparatus under N₂ atmosphere (20 ml.min⁻¹) at the rate of 10 °C/min and with weight samples equal to 10 mg.

The solvent uptake measurements were done according to the gravimetric method (ASTM D 2765-95, Method C). The samples (circular film having 1mm thickness obtained by compression moulding) were immersed in toluene for 3 days at 25 °C. The results were averaged for five measurements.

DSC measurements (melting behaviour) were carried out under nitrogen gas on a DSC 2920 TA instruments apparatus interfaced with computer. For each formulation, samples of 10 mg weight were analyzed. Two measurements were done under nitrogen atmosphere with a heating rate of 10 °C/min. For better precision, only the second measurement was taken into account. The following analysis program was applied: cooling from room temperature to -100 °C at 10 °C/minute, afterwards, holding at -100 °C for 10 minutes, then heating to 250 °C at 10 °C/minute, and finally, holding at 250 °C for 10 minutes.

The rheological analysis was done with a Monsanto Rheometer, model 100/4308, in order to get the exerted torque versus time. For each formulation, samples of 4.5 g weight were analyzed under temperature equal to 175 °C.

3. Results and discussion

3.1. XRD analysis (WAXD)

From Fig 1a it can be noted that for neat clay, the (001) plane diffraction peak is located at $2\Theta = 2.75^\circ$, this value, according to Bragg's law, corresponds to 3.21 nm interlayer spacing. The presence of four peaks between 14 and 20° , in Fig 1b, can be explained by the crystalline structure of PP chains [18-19]. The peaks at 14.1° , 16.8° and 18.5° due to the (110), (040) and (130) planes are characteristics of α -type monoclinic crystal structures of PP chains [18-19]. The peak at 16.2° (indicated by a vertical arrow in Fig 1b) is due to (300) reflection plane of β -type hexagonal crystal structure of PP chains [18-19]. For 3 wt % organoclay loading, the (001) plane diffraction peak is shifted toward low angles at $2\Theta = 2^\circ$ ($2\Theta = 2.75^\circ$ is indicated by a vertical line in Fig 1d, the shifted peak is indicated by a vertical arrow in Fig 1d and a magnification of this peak is clearly showed in Fig 1h). The value, $2\Theta = 2^\circ$, according to Bragg's law, corresponds to 4.41 nm interlayer spacing.

The shift towards low angles of the (001) clay peak can be explained by an increase of the interlayer distance of clay platelets due to intercalation of blend chains. For formulations containing 7 wt % and 9 wt % organoclay, represented, respectively, by Fig 1f and Fig 1g, we can observe that the (001) diffraction peak remains unchanged and it is located at $2\Theta = 2.75^\circ$. For blends containing 1, 3 and 5 wt % organoclay, it can be seen that the β phase characteristic peak has been reduced in intensity (Fig 1c) or disappeared (Fig 1d and Fig 1e); this can be explained by the fact that the intercalated component NR prevents the crystal growth of the β phase inside clay galleries; and therefore, the intercalated amorphous NR do not possess a nucleating effect for the β phase. In other cases, the intercalated component can possess a nucleating effect for the β phase, as it was observed for PP-g-SBR particles which promote the β crystal growth of PP in the PP/PP-g-SBR nanocomposite blend [19]. A similar trend (elastomeric phase obstructs the mobility of PP chains and hence affect the PP crystallisation) was also reported [20-22].

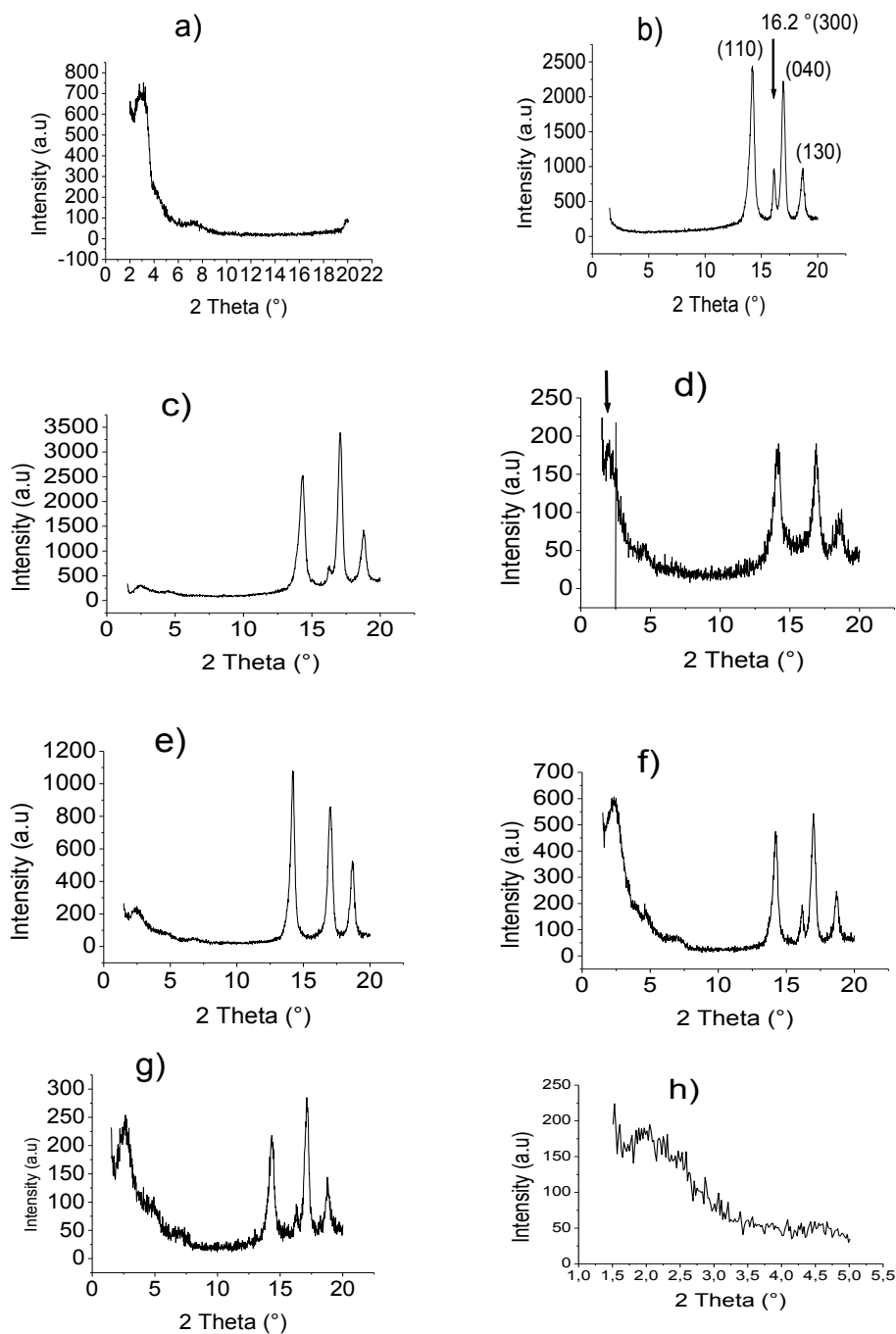


Fig. 1. XRD patterns of: (a) organoclay (OMMT), (b) Pure polypropylene, (c) PP/NR/OMMT (89.1/9.9/1), (d) PP/NR/OMMT (87.3/9.7/3), (e) PP/NR/OMMT (85.5/9.5/5), (f) PP/NR/OMMT (83.7/9.3/7), (g) PP/NR/OMMT (81.9/9.1/9), (h) PP/NR/OMMT (87.3/9.7/3) a magnification of the shifted peak

3.2. Mechanical properties

It can be observed from Table 1, that the adding of 10 wt % of NR to PP induces a decrease of the maximal tensile strength, shore A hardness and it induces also an increase of the elongation at break. So, the incorporation of NR to PP induces a decrease of the stiffness, strength and improves the ductility of the resulting blend. These results can be explained by the soft nature of the NR when it is added to the PP more rigid phase [17]. Moreover the 3 wt % organoclay based composite has the highest tensile strength, hardness, elongation at break and impact strength (toughness). A maximal tensile strength for a certain nanofiller concentration was observed in nanocomposite systems [22-25]. A maximal tensile strength and a maximal elongation at break for a certain nanofiller concentration was also observed in a nanocomposite system [26]. The existence of organoclay agglomerates is believed to reduce the tensile elongation, this is because the agglomeration of the organoclay can act as a stress concentration point and consequently increase the ability of the composite to initiate cracks [27].

Table 1. Mechanical properties values of neat PP, PP/NR (90/10) blend and its nanocomposites

Sample	NR (wt %)	Organoclay (wt %)	Tensile strength (MPa)	Shore A hardness	Elongation at break (%)	Izod impact strength (kJ/m ²)
PP	0	0	29.54	96.90	6.00	18.00
PP/NR/OMMT (90/10/0)	10	0	22.17	94.75	20.24	39.96
PP/NR/OMMT (89.1/9.9/1)	89.1	1	22.57	96.25	24.10	55.10
PP/NR/OMMT (87.3/9.7/3)	87.3	3	24.35	98.10	27.66	81.80
PP/NR/OMMT (85.5/9.5/5)	85.5	5	19.08	96.10	26.30	37.47
PP/NR/OMMT (83.7/9.3/7)	83.7	7	22.56	96.15	25.54	27.50
PP/NR/OMMT (81.9/9.1/9)	81.9	9	22.33	96.00	12.23	14.70

It can be observed from Table 1 that the 3 wt % loading organoclay blend possesses balanced mechanical properties, i.e., the stiffness (expressed by the tensile strength and hardness) as well as the ductility (expressed by the elongation at break and impact strength) are maximal. The maximal values of tensile strength, hardness, elongation at break and impact strength obtained for 3 wt % organoclay loading can be explained by the intercalation of the PP/NR chains between organoclay platelets as evidenced by XRD analysis.

The improvements (up to 3 wt % organoclay loading) of tensile strength and hardness show that organoclay acts as reinforcing filler. The increase of elongation at break and impact strength (up to 3 wt % organoclay loading) can be explained by the improvement of the ductility due to the compatibilization effect of the organoclay [6]. The improvements of the mechanical properties, up to 3 wt % organoclay loading, can be explained by the two step processes used in the present study (extrusion followed by compression moulding) since it has been reported that such two step process can improve notably the properties of composites [28]. Since rubber toughening is accompanied by an increase in toughness and ductility and a reduction in material stiffness, strength and hardness; therefore, in the present study, the inclusion of 3 wt % organoclay rigid filler leads to a better balance between strength and ductility.

3.3. Morphological study

It can be noted from Fig 2a that, when the organoclay is not added, the rubber domains easily debonded from the polypropylene matrix due to the poor interfacial adhesion between them (In Fig 2, typical rubber domains are inside circles indicated by arrows). Furthermore, in Fig 2a, the average rubber domains size is about 25 μm , and the spatial distribution of these domains into polypropylene matrix is not uniform. Fig. 2b shows that, when 1 wt % of organoclay is added, the rubber average interparticle distance decrease and the average size of the dispersed rubber phase is found to be about 10 μm . Khatua et al. [29] have reported similar observation in their study on PA6/EPR nanocomposites where domain size of EPR decreased even when a small amount (1 wt %) of organoclay was added. Fig. 2c shows that the average rubber domain size reduced to about 5 μm when the concentration of the organoclay is equal to 3 wt %; and the distribution of these rubber domains into matrix becomes more homogenous relatively to the case in which the concentration is equal to 1 wt % (Fig 2b). At 3 wt % organoclay concentration, droplet-like dispersion morphology is observed with low coalescence and a narrow distribution of the rubber particle sizes. This phenomenon can be explained by the compatibilization effect of the organoclay as previously reported [30]. Figs 2d, 2e and 2f show that when the organoclay concentration is greater than 3 wt %, the rubber domain sizes increase and their distribution in the matrix becomes not uniform indicating a weak interfacial adhesion with polypropylene matrix and a tendency towards coalescence. Furthermore, Fig. 2a shows that the clay agglomerates (white particles) have the lowest size and are distributed homogenously only for 3 wt % organoclay loading (Fig 2c); this explains the highest value observed for tensile strength at this concentration.

It can be also observed from SEM micrographs that as the organoclay content increases (greater than 3 wt %), some organoclay particles begin to aggregate (the white particles in Figs 2b, 2c, 2d, 2e and 2f are organoclay aggregates). It can also be noted from Figs 2b, 2c, 2d, 2e and 2f that the organoclay is distributed in the PP matrix only like aggregates because in the present study a compatibilizing agent was not used. This observation can be supported by the decrease of the tensile strength (observed for organoclay concentration greater than 3 wt %) which can be explained by the weak interaction between PP and organoclay filler as it was previously reported [31]. The formation of these organoclay aggregates reduces the interfacial area between the polymers and organoclay layers, which leads to lower mechanical properties [27]. Fig 3a shows that deformation occurred at the interface between PP matrix and rubber particles forms fibril-like structures (see arrow A). The observation of these fibrils indicates the improvement in toughness of the blend [32-33]. The formation of the elongated fibril-like structures can explain the higher tensile properties of the nanocomposite at 3 wt % organoclay loading. Fig 3b shows NR particles (see arrow B) dispersed in the PP matrix. This figure shows that the organoclay (lightest areas) is located at the external surface of NR dispersed particles rather than in the bulk PP matrix. This figure shows that, the organoclay is located at the interface, or interphase, between PP matrix and NR particles and also it is embedded or encapsulated in the bulk of NR particles. The location of the organoclay can explain the compatibilization and reinforcement effect of organoclay since the location of the filler at the interface has a great influence on the blend performance [34].

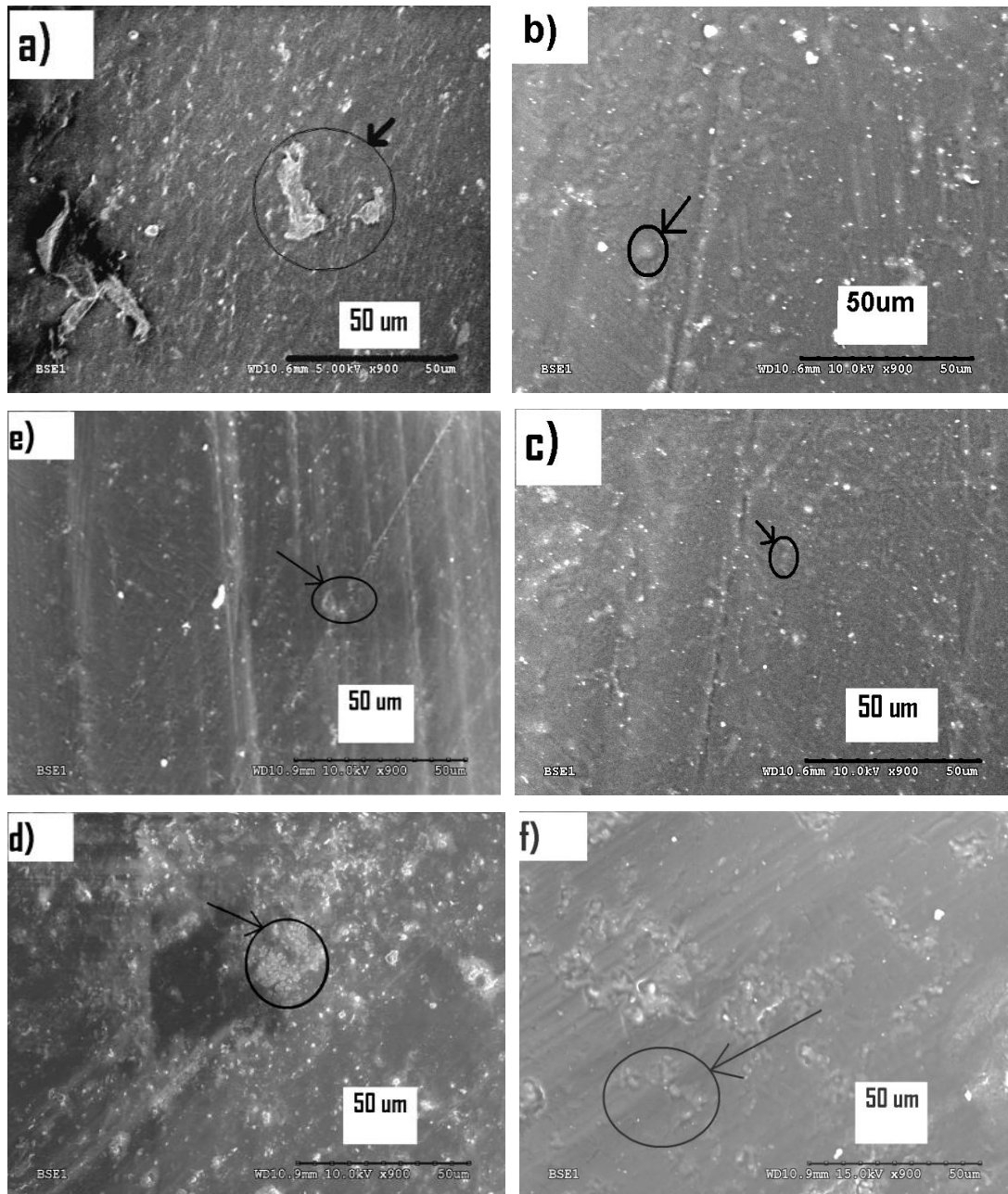


Fig. 2. SEM micrographs (taken in BSE mode) showing the fractured surfaces of : (a) neat polypropylene /natural rubber blend (90/10/0), (b) PP/NR/OMMT (90/10/1), (c) PP/NR/OMMT (87.3/9.7/3), (d) PP/NR/OMMT (85.5/9.5/5), (e) PP/NR/OMMT (83.7/9.3/7), (f) PP/NR/OMMT (81.9/9.1/9)

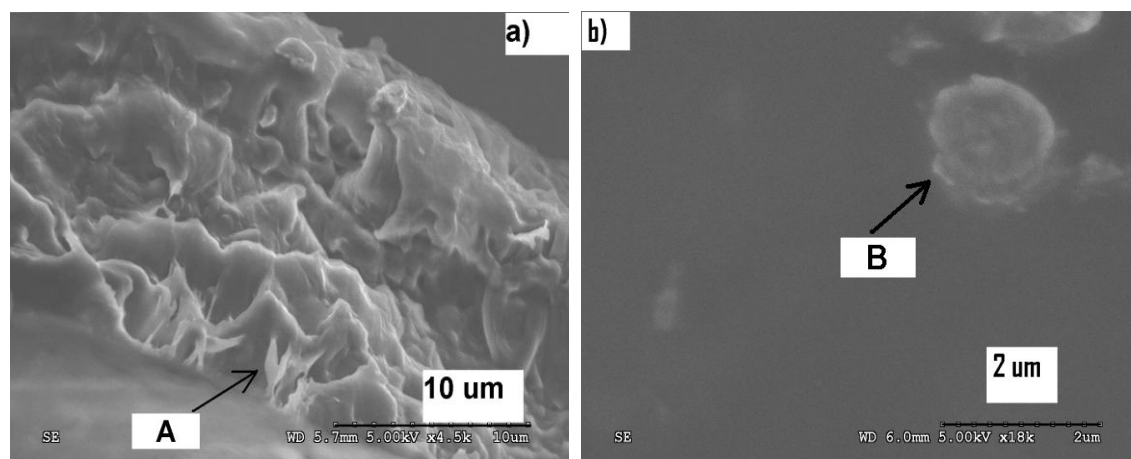


Fig. 3. SEM micrographs at low magnification (taken in SE mode) showing the fractured surfaces of: PP/NR/OMMT (87.3/9.7/3) blend.

The location of the organoclay between PP and NR phases can be explained by the compatibilizer role of organoclay because the compatibilizer can recover the dispersed domain as it was noticed for PP-g-MA in PP/PET/OMMT nanocomposite [35]. On the other hand, it was also reported that the size reduction of the dispersed phase can be related to the location of the organoclay in the interfacial region that may act as a compatibilizer and hinder the coalescence of the dispersed phase [35]. The organoclay acting as a compatibilizer, located in the interphase, may act as an adhesion promoter between the PP and NR phases.

3.4. Thermal analysis

The information that seems to be important to characterize thermal stability is the onset temperature of the degradation, which is measured both by the temperature at which 5 wt % degradation occurs ($T_{5\%}$), the mid-point of the degradation ($T_{50\%}$), and the fraction which is not volatile at 600 °C, denoted as char residue [36]. The curves obtained by thermogravimetric analysis are shown in Fig 5, and their related results are summarized in Tab 2. In the TGA curves, one can see that there is one step in the degradation of polypropylene/natural rubber blend and its nanocomposites. This degradation can be explained by the polypropylene and natural rubber main chain pyrolysis as reported in the literature [37].

The TGA curves show that after pyrolysis, the clay based composites form a larger char residue than the neat polypropylene/natural rubber blend, especially for formulations containing 5, 7 and 9 wt % organoclay loading. Therefore, the introducing OMMT enhances the formation of a char on the surface of polypropylene/natural rubber blend and, as a consequence, reduces the rate of decomposition of the clay based composites.

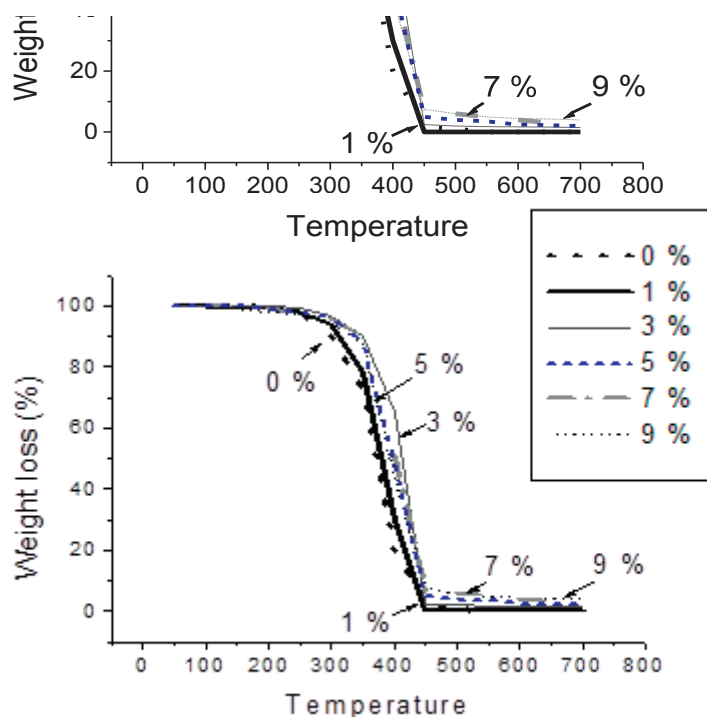


Fig. 4. TG thermograms of PP/NR blend (0 % OMMT) and its nanocomposites.

It can be clearly observed, from fig 4 and Table 2, that the formulation containing 3 wt % of organoclay possesses the highest thermal stability because the onset degradation temperature ($T_{5\%}$) and the mid-point degradation temperature ($T_{50\%}$), are highest relatively to the other formulations. It can be noted, from Table 2, that formulation in which the organoclay concentration is 3 wt % possesses the highest thermal stability because at 400 °C this formulation presents 35 wt % in weight loss and the other formulations present more weight loss at this temperature. On the other hand, Fig 4 shows clearly that the 3 wt % organoclay based blend is, between 50°C and 450 °C, the more thermally stable since it presents less weight loss; this is due to the high degradation resistance of the intercalated-confined blend chains and also to the reduction of the diffusion rates of volatiles out of the material [37].

Table 2. TGA results for PP/NR (90/10) blend and its nanocomposites.

Organoclay content (%)	$T_{5\%}$ (°C)	$T_{50\%}$ (°C)	Char residue (%) obtained at 600 °C	Weight loss value (%) occurred at 400 °C
0	270	375	0	70
1	280	380	1	80
3	330	425	3	35
5	325	410	5	49
7	325	410	6.7	50
9	285	400	8.5	56

3.5. Rheological study

Many researchers [33] reported that Brabender torque –time curves can be used to analyse the processing characteristics of polymer melt mixing. The equilibrium torque (stabilization torque) reached at the completion of melt mixing was used to assess the processability of the polymer mixing which is related directly to the viscosity of the blend [38-39]. On the other hand, the maximal torque (MH) can be regarded as a measure of the blend stiffness or Young's modulus [40], and the minimal torque (ML) is related to the melt viscosity of the blend [40]. Fig.5 shows the plastograms of pure PP/NR blend and PP/NR//OMMT nanocomposites and their related results are summarized in Tab 3. It can be deduced from fig 6 and table 3 that the incorporation of organoclay has increased the MH and MH-ML difference, whereas, the ML remains constant on the whole (approximately 3 dN.m). It can be noted that, for all formulations, the introduction of organoclay into the PP/NR blend has not increased the torque in the steady state (BT). Furthermore, the melt viscosity, expressed by ML [40] and BT [38-39], of organoclay based formulations does not increase relatively to the pure PP/NR one. It can be concluded that the processability of the PP/NR blend is not notably affected by the addition of the organoclay, and thus, the decrease of the rubber domain sizes observed by SEM is not due to the increase of the blend melt viscosity [7].

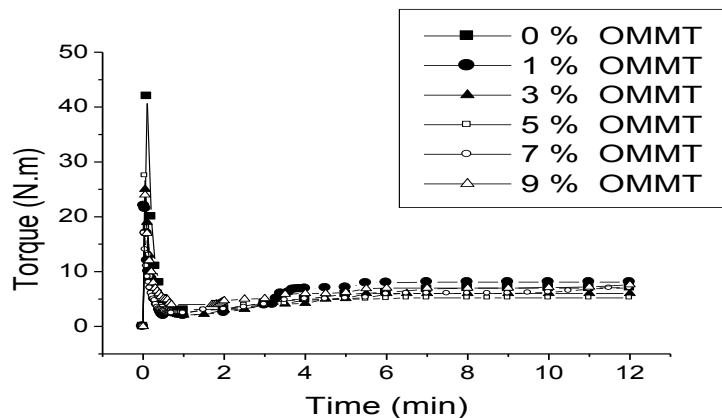


Fig. 5. Torque versus time of pure PP/NR blend (0 % OMMT) and its nanocomposites.

Table 3. Torque maximum (MH), torque minimum (ML), torque difference (MH-ML) and balanced torque (BT) versus time for PP/NR (90/10) blend and its nanocomposites.

Organoclay content (phr)	MH (dN.m)	ML (dN.m)	MH-ML (dN.m)	BT (dN.m)
0	16.5	2.5	14.0	7.0
1	22.0	2.0	20.0	8.0
3	24.0	4.0	20.0	7.5
5	25.0	2.5	22.5	6.0
7	27.5	2.5	25.0	5.5
9	42.0	2.9	39.1	7.0

The significantly increased values in MH with organoclay loading are due to the increase of the stiffness or Young's modulus of the blend [40]. These increased values in MH are indirect hint for improved interaction behaviour and good interfacial adhesion between matrix and filler. Indeed, for strongly binding polymers to filler surface there will be an area of high density and thus, high modulus forms next to the surface. Thus if all areas of the filler surfaces are capable of adsorption (high interaction), the segment of polymer chains will be absorbed on the surfaces and form a flat and dense layer close to the filler surfaces. This area will have combination properties of fillers (great modulus) and matrix [41]. It can be noted from Table 3 that the MH-ML increases as a function of the organoclay loading. The MH-ML is a measure of the dynamic shear modulus, which indirectly relates to the crosslink density of the nanocomposite [42]. The crosslink resembles a three dimensional network in the composite [42]. Thus, it can be reasonably assumed that this three dimensional network is formed by organoclay platelets embedded in the NR phase since SEM analysis has revealed that organoclay platelets are mainly located at the PP/NR interface and embedded in the NR phase.

3.6. Solvent resistance properties

The results of the solvent uptake measurement are shown in Tab 4. It can be seen that the formulation containing 3 wt % of organoclay presents the lowest solvent uptake rate or the lower solvent permeability. The decrease of the solvent uptake for a thermoplastic elastomer reinforced with organoclay was previously reported [23].

Table 4. Solvent resistance properties (measured in toluene at 25 °C for 3 days) ^a of PP/NR (90/10) blend and its nanocomposites

Organoclay content (phr)	Solvent uptake rate (wt %)
0	9.28
1	9.00
3	7.80
5	8.14
7	14.84
9	16.20

^a The solvent uptake rate was calculated as follow [23]:
 solvent uptake rate = $(W_2 - W_1) / W_1 \times 100\%$, where W_2 is the weight of the wet sample and W_1 is the weight of the dry sample.

The decrease of the gas (CO_2 and O_2) permeability for a certain organoclay concentration (5 wt %) in a PP/EPDM thermoplastic elastomer blend was also reported [33]. In the present study, the decrease of the solvent uptake is due to the efficient barrier effect of the organoclay [33]. This result can be explained by the intercalation of blend (PP/NR) chains between clay platelets. This intercalation leads to the formation of a bound polymer in close proximity to the reinforcing organoclay which restricts the solvent uptake [23]. The increase of the solvent uptake as the organoclay content becomes greater than 3 wt % can be explained by the aggregation of the organoclay particles. The formation and the increase of these organoclay aggregates facilitate the permeation of the solvent and as a consequence increase its uptake effect

3.7. DSC analysis (melting behaviour)

The DSC thermograms are represented in Fig 6 and their related results are summarized in table 5. Figure 6 shows the peak related to the melting temperature of polypropylene phase. It can be noted from Fig 6 that for formulations containing 0, 1, 5, 7 and 9 wt % of organoclay, the melting temperature of the polypropylene phase remains constant and is equal to 169 °C. When the concentration of the added organoclay becomes equal to 3 wt %, the melting temperature of the polypropylene phase decrease decreased to 162 °C. A decrease of the melting temperature of the matrix was observed for polyamide 66/clay nanocomposites [43], and this decrease was related to the reduction in crystallite size in the presence of filler [38]. A decrease of the melting temperature of the PP matrix was equally observed for PP/bentonite composite [27], PP/ SiO_2 nanocomposite [44] and PP/PET/OMMT nanocomposite [35].

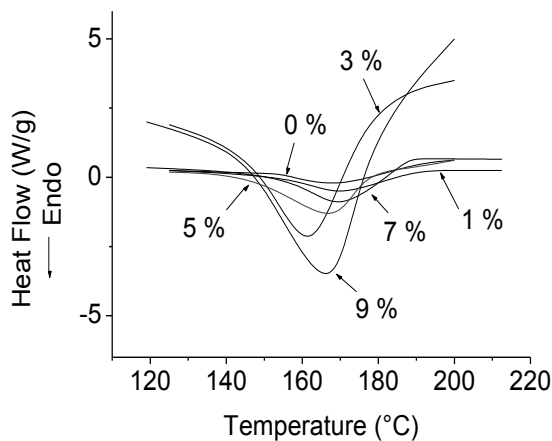


Fig. 6. DSC thermograms of pure PP/NR blend (0 % OMMT) and its nanocomposites

Table 5. Melting temperature of PP phase (T_{pp}^m) in PP/NR/OMMT blend, versus the organoclay content.

Organoclay content (wt %)	T_{pp}^m (°C)
0	169
1	169
3	162
5	169
7	169
9	169

For formulation containing 3 wt % of organoclay, the decrease of the polypropylene crystallite size (as evidenced by the decrease of the PP phase melting temperature) improves the toughness of the blend as it was previously reported [45]. In the present study, the decrease of the polypropylene melting temperature can be explained by the reduction in crystallite size due to the intercalation of the NR chains with PP macromolecules between clay platelets. Indeed, the presence of an elastomeric phase can decrease the melting temperature of the PP phase as it was noticed for PP/PP-g-SBR nanocomposite [19]. A similar trend, i.e. an intercalation of a rubbery component with polypropylene between organoclay platelets, was also reported by George and co-workers [46].

On the other hand, the decrease of the PP melting temperature in the blend can also be attributed to a strong interaction of the organoclay filler with PP phase, as it was noticed for the decrease of EVA melting temperature in PP/EVA/WP system [31]. This strong interaction of the organoclay filler with PP phase can be explained by the intercalation of the PP chains between organoclay platelets as evidenced by XRD analysis. Since organoclay platelets can be intercalated simultaneously by polypropylene and natural rubber chains, this simultaneous intercalation can be explained by the fact that the intercalated organoclay platelets are located at the interface, between rubber domain and polypropylene phase and, as a consequence, the platelets act as a compatibilizer between these two phases. The PP and NR chains co-intercalate, in the same space gallery, between the organoclay platelets and they expand them partially so that the total exfoliation does not occur [47]. This location of the filler at the interface, between two components in a polymeric blend, was also reported [31, 34-35, 48].

4. Conclusion

In this study it was observed that the improvements of the mechanical, thermal, morphological and solvent uptake properties of the prepared blend are realised for 3 wt % organoclay loading. The stiffness (expressed by the tensile strength and hardness) and ductility or toughness (expressed by the elongation at break and impact strength) are well balanced for 3 wt % organoclay concentration.

The XRD analysis showed that, at 3 wt % organoclay loading, the macromolecular chains of the blend were intercalated in the interlayer space of the organoclay platelets; and the intercalation of the rubber phase causes the disappearance of the PP β crystalline phase.

The SEM and TOM studies revealed that at 3 wt % organoclay loading there is a decrease of the rubber domain and organoclay agglomerate sizes. The SEM study has revealed that at 3 wt % organoclay loading the rubber particles present suitable sizes uniformly distributed for effective toughening, and at this

concentration the organoclay is located at the PP/NR interface and is embedded in the NR phase. The DSC study confirmed a simultaneous intercalation of rubber chains with polypropylene macromolecules between organoclay platelets. The rheological study revealed that the viscosity of the studied formulations does not increase with the addition of organoclay and the organoclay platelets dispersed inside NR phase form a three dimensional network. The major finding of this study is that for the PP/NR (90/10) blend, the stiffness and toughness are well balanced for 3 wt % organoclay loading and the compatibilization and reinforcement effects of the organoclay are highest for the same concentration.

References

- [1] Alexandre M, Dubois P. *Mater. Sci. Eng.* 2000; **28** :1-63.
- [2] Bergman J S, Chen H, Giannelis E P, Thomas M G, Coates G W. *Chem. Com.* 1999 ;**21** : 2179-2180.
- [3] Giannelis E. P, Krishnamoorti R, Manias E. *Adv. Polym. Sci.* 1999; **138** :107.
- [4] Chen T K., Tien Y I, Wei K. H, *Polym. Sci. Part A: Polym. Chem.* 1999;**37**: 2225.
- [5] Voulgaris D, Petridis D. *Polymer* 2002; **43**; 2213.
- [6] Gelfer M Y, Song H H., Liu L, Hsiao B S, Chu B, Rafailovich, M. *J. Polym. Sci. Part B: Polym. Phys.* 2003; **41**: 44.
- [7] Ray S. S., Bousmina, M, Proceedings of the 23rd annual meeting of Polymer Processing Society, PPS-23, pp 8, Salvador, Brazil, 27th-31th May (2007).
- [8] Zhu S H, Chan C M, Zhang Y X, *J. App. Polym. Sci.* 1995 ; **58**: 621.
- [9] Oh J. S, Isayev A. I, Rogunova M. A, *Polymer* 2003; **44**: 2337-2349.
- [10] Premphet K, Horanont P. *Polymer* 2000; **41**: 9283-9290.
- [11] S. Duquesne, Jama C, leBras M, Delobel R, Recourt P, Gloaguen J. M, *Comp. Sci.. Tech.* 2003 ; **63** : 1141-1148.
- [12] Primet, R. *Des plastiques techniques*, Rhone Poulenc, Paris : Techno Nathan ; 1990.
- [13] Hanafi I, Suryadiansyah S. *J. Reinf. Plast. Comp.* 2004; **23**(6): 639-650.
- [14]. Wahit M. U, Hassan A., Mohd Ishak Z. A, Czigany T., *Exp. Polym. Lett.* 2009; **5**(3): 309-319.
- [15] Van der Wal A, Mulder J. J, Oderkerk J., Gaymans R. J, *Polymer* 1998; **39**: 6781-6787.
- [16] Gonzales I., Eguiazabal J. I., Nazabal J, *Europ. Polym. J.* 2008; **44**: 287-299.
- [17] Lim J W, Hasan A, Rahmat A R, Wahit M U, *J. App. Polym. Sci.* 2003; **99**: 3441-3450.
- [18] Lipponen S, Pietikäinen P, Vainio U, Serimaa R, Seppälä J V, *Polym. & Polym. Comp.* 2007; **15**(5): 343-355.
- [19] Wang W, Fu M, Qu B, *Polym. Adv. Tech.* 2004; **15**:467.
- [20] Arroyo M, Zitzumbo R, Avalos F, *Polymer* 2000; **41**: 6351.
- [21] Yu J, Wang G, Chen J., Zeng X, Wang W. *Polym. Eng. Sci.* 2007; **40**; 201.
- [22] Xiao M., Sun L, Liu J., Li Y, Gong K, *Polymer* 2002 ; **43** : 2245.
- [23] Mishra J. K., Kim G, Kim I, Chung I. J, Ha C. S, *J. Polym. Sci.: Part B: Polymer Phys.* 2004; **42**: 2900.
- [24] Hwang W. G., Wei K. H., Wu C. M, *Polymer* 2004; **45**: 5729.
- [25] Sharif J, Yumus W. M. Z, Dahlan K. H, Ahmad M. H. J. *App. Polym. Sci.* 2006;**100**: 353-362.
- [26] Kotal M, Srivastava S. K, Bhowmick A. K. *Polym. Int.* 2010; **59**: 2-10 .
- [27] Othman N, Ismail H, Mariatti M. *Polym. Deg. Stab.* 2006; **91**: 1761.
- [28] Mina F, Seema S, Matin R, Rahaman J, Sarker R. B. Gafur A, Bhuiyan A. H. *Polym. Degrad. Stab.* 2009; **94**: 183-188.

- [29] Khatua B. B, Lee D. J, Kim H. Y, Kim J. K. *Macromolecules* 2004 ;**37** : 2454-2459.
- [30] Tabtiang A, Lumlong S, Venables A, *Polym. Plast. Tech. Eng.* 2000 ; **39** : 293.
- [31] Dikobe D. G, Luyt A. S. *Exp. Polym. Lett.* 2009; **3**(3):190-199.
- [32] Gonzalez-Montiel A, Keskkula H, Paul D. R. *J. Polym. Sci.: Part B: Polym. Phys.* 1995; **33**: 1751-1767.
- [33] Frounchi M, Dadbin S, Salehpour Z, Noferesti M, *J. Memb. Sci.* 2000;**282**:142-148.
- [34] Wu D, Yisheng Z, Zhang M, Yu W. *Biomacromolecules* 2009; **10**: 417-424..
- [35] Calcagno C. I. W, Mariani C. M, Teixeira S. R, Mauler R. S. *J. App. Polym. Sci.* 2009; **111**: 29-36.
- [36] Zong R, Hu Y, Wang S, Song L. *Polym. Deg. Stab.* 2004; **83**: 423-428.
- [37] Gilman J. W. *Chem. Mater.* 2002; **12**: 1866-1873.
- [38] Blyler L. I., Dane J. H. *Polym. Eng. Sci* 1967; **7**: 178-181.
- [39] Goodrich J. E, Porter R. S. *Polym. Eng. Sci.* 1967; **7**: 45-51.
- [40] Teh, J P. L, Mohd Ishak, Z. A, Hashim A. S, Kager-Kocsis J, Ishiaku U. S. *Euro. Polym. J.* 2004; **40**: 2513-2521.
- [41] Mohamad N, Muchtar A, Ghazali M. I, Mohd D. H, Azhari C. H. *Euro. J. Sci. Res.* 2008; **24**(4):538-547.
- [42] Ismail H, Chia H. H. *Euro. Polym. J.* 1998; **34**(12): 1857-1863.
- [43] Li X, Wu Q, Berglund L. A. *Polymer* 2002;**43**:4967-4972.
- [44] Garcia M, Van Vleet G, Jain S, Schroyen B A G, Sarkissov A, Van Zyl W. E, Boukamp B. *Rev. Adv. Mater.* 2004; **6**:169-175.
- [45] Song K. *App. Polym. Sci.* 2000; **78**: 412-423.
- [46] George S, Varughese K. T, Thomas S. *Polymer* 2000; **41**: 5485.
- [47] Bendjaouahdou C, Bensaad S. *J. Vinyl. Addit. Technol.* 2011; **17**:48–57.
- [48] Fang Z, Xu Y, Tong L. *Polym. Eng. Sci.* 2007; **46**: 551-559.

